

Research Paper

Gain of a 500-fold sensitivity on an intravital MR Contrast Agent based on an endohedral Gadolinium-Cluster-Fullerene-Conjugate: A new chance in cancer diagnostics

Klaus Braun¹✉, Lothar Dunsch², Ruediger Pipkorn³, Michael Bock¹, Tobias Baeuerle¹, Shangfeng Yang^{2,4}, Waldemar Waldeck⁵ and Manfred Wiessler¹

1. Department of Medical Physics in Radiology, German Cancer Research Center, INF 280, D-69120 Heidelberg, Germany
2. Department of Electrochemistry and conducting Polymers; Leibniz-Institute for Solid State and Materials Research, Helmholtzstraße 20, D-01069 Dresden, Germany
3. Core Facility Peptide Synthesis, German Cancer Research Center, INF 580, D-69120 Heidelberg, Germany
4. Hefei National Laboratory for Physical Sciences at Microscale & Department of Materials Science and Engineering, Hefei 230026, China
5. Biophysics of Macromolecules, German Cancer Research Center, INF 580, D-69120, Heidelberg, Germany

✉ Corresponding author: Dr. Klaus Braun, Im Neuenheimer Feld 280, German Cancer Research Center, Dep. Of Medical Physics in Radiology, D-69120 Heidelberg, Germany. Tel. No.: +49 6221 42 2495; Fax No.: +49 6221 42 3326; E-mail: k.braun@dkfz.de

Received: 2010.03.12; Accepted: 2010.05.26; Published: 2010.05.28

Abstract

Among the applications of fullerene technology in health sciences the expanding field of magnetic resonance imaging (MRI) of molecular processes is most challenging. Here we present the synthesis and application of a $Gd_xSc_{3-x}N@C_{80}$ -BioShuttle-conjugate referred to as **Gd-cluster@-BioShuttle**, which features high proton relaxation and, in comparison to the commonly used contrast agents, high signal enhancement at very low Gd concentrations. This modularly designed contrast agent represents a new tool for improved monitoring and evaluation of interventions at the gene transcription level. Also, a widespread monitoring to track individual cells is possible, as well as sensing of microenvironments. Furthermore, BioShuttle can also deliver constructs for transfection or active pharmaceutical ingredients, and scaffolding for incorporation with the host's body. Using the Gd-cluster@-BioShuttle as MRI contrast agent allows an improved evaluation of radio- or chemotherapy treated tissues.

Key words: inverse Diels Alder Reaction, BioShuttle, fullerenes, gadolinium, intravital Imaging; nitridecluster fullerenes; intracellular imaging, Magnetic Resonance Imaging (MRI), metallofullerenes, Molecular Imaging; Rare Earth compounds

Introduction

Since Kraetschmer's pioneering work in the synthesis of fullerenes[1, 2] continued the initial work by Kroto, Smalley and Curl[3-5], speculations for possible applications were tremendous, after the successful large-scale synthesis and the characterisation of the structural and electronic properties of the fullerenes.[6,7] Endohedral fullerenes (endofullere-

nes) can trap atoms, ions or clusters, such as the Gadolinium ions (Gd^{3+}) inside their inner sphere. In most endofullerenes a charge transfer from the incorporated species unto the cage occurs, resulting in a more polar molecule.[8]

The hydrophobic character of fullerenes was compromised by covalent addition of hydrophilic

groups at the cage's surface. The synthesis of such a fullereneol was first reported by Chiang et al. in 1992.[9] The continuous attention which fullereneols attracted since then was largely due to their hydroxyl groups resulting in increased water solubility. The modification of lipophilic fullerenes to become water-soluble was used for endohedral metallofullerenes permitting multi-faced applications also dedicated for industrial use.[10, 11] Such molecules were selected to carry active agents or diagnostics into the organism. Their paramagnetic properties differ dramatically from the commonly used diagnostic routine tools, in which Gd^{3+} is bound to chelating agents like diethylenetriaminepentaacetic acid (DTPA) (Magnevist®), or diethylenetriamine-pentaacetate-bis-(methylamide) (Omniscan®), or 1,4,7-tris-(carbonyl-methyl)-10-(2'-hydroxypropyl)-1,4,7,10-tetraazacyclodecane (Prohance®).[12, 13]

Biochemical safety studies for adverse reactions such as nephrogenic fibrosis by using Gd-based intravascular contrast agents are suggestive.[14] In order to meet these higher requirements for intracellular magnetic resonance tomography (MRT) contrast agents, the development of functional molecules must feature both: the complete lack of Gd^{3+} ion-release under metabolic processes and no detection by the reticulo-endothelial system (RES). Such contrast agents (CA) have the potential for a successful real-time *in vivo* imaging of intracellular processes. The development of water-soluble fullerenes with surface modifications like polyamido-amine dendrimers bearing cyclodextrin (CD) or polyethylene glycol (PEG) and Gd-metallofullerenes [$Gd@C_{82}(OH)_n$, Gd-fullereneols] seems to be a feasible approach for the use as a diagnostic tool in MRI.[15] However, there is evidence that $Gd@C_{82}(OH)_n$ tends to be entrapped in the RES by forming large particles interacting with plasma components like albumin,[16] whereas $Gd@C_{60}[C(COOCH_2CH_3)_2]_{10}$ lacks an accumulation in the RES system.[17] [18] [19, 20] Here we focus on the selective development of nitride cluster fullerenes of Gd (and additional rare-earth elements featuring dipoles like Yttrium [Yt], Scandium [Sc]), such as $Gd_nSc_{3-n}N@C_{80n}$ [21], which was recently characterized by the Dunsch group.[22] We considered these molecules for molecular imaging (MI) to depict morphological structures in an outstanding manner. MI is defined as the characterization and measurement of biological processes at the cellular and molecular level.[23] At present the rapidly emerging field of successful MI is represented by positron emission tomography (PET)[24], possibly combined with computer tomography (CT)[25] or combined with single photon emission computed to-

graphy (SPECT)[26] as well as bioluminescent (Blm)[27] and fluorescent imaging (Flm)[28]. Both modalities are still restricted to small-animal use.[29] While MRT reveals morphological structures in soft tissue with low intrinsic sensitivity, the sensitivity of PET is unmatched but hampered by the dependence on suitable PET tracers. Its disadvantages include non-detectable "low grade" tumors, false-positive results and radiation exposure.

Requirements for successful intracellular imaging with MRT are a perspicuous signal and a sufficient accumulation of contrast agent (CA) within the target cells. There are numerous approaches[30, 31] but further developments of MR contrast agents with new properties are indispensable. All CAs used so far including the prospective $Gd_xSc_{3-x}N@C_{80}$ offer one feature in common: they are not able to penetrate the cellular membranes and their use is restricted to the blood stream and the interstitial space. The use of transfection agents facilitating the passage of Gd-containing endofullerenes across the cell membrane into the cytoplasm was described [15] but is critical, or even toxic.

To circumvent these biological hurdles we pursued another solution for our "cell-nucleus imaging". For a successful intracellular and intranuclear MRI we covalently linked $Gd_xSc_{3-x}N@C_{80}$ molecules with both the nuclear address (NLS) derived from SV40 T-antigen[32], which in turn is linked via a disulfide-bridge to a peptide facilitating the passage across cell membranes (CPP)[33]. This is our BioShuttle-conjugate resulting in a Cell Nucleus (NLS)- $Gd_xSc_{3-x}N@C_{80}$. For simplification in the text it is called Gd-cluster@-BioShuttle utilizing the cytoplasmically located importins, classified as substrates for the active RAN-GDP system, mediating an efficient transport of the $Gd_xSc_{3-x}N@C_{80}$ cargo into cell nuclei.[34]

To build such conjugates we improved methods for rapid and complete ligation of hydrophobic molecules like fullerenes (and especially their functionalized derivatives) to carrier molecules. In our studies, the Diels-Alder-Reaction (DAR) turned out to be an applicable ligation method, but the reverse reaction proved to be restrictive and unsatisfactory.[35] The use of the "DAR with an inverse electron demand (DAR_{inv})" can circumvent these drawbacks and has been accurately described.[36-38]

In this paper, we exemplarily demonstrate a successful intracellular MRI through a novel CA-delivery. Due to its higher sensitivity an imaging of previously non-detectable micro-metastases and cell trafficking patterns is possible.

Chemical Procedures

The synthesis and isolation of the $Gd_xSc_{3-x}N@C_{80}$ cluster fullerenes has been described elsewhere.[22] All chemical reactions and procedures were carried out under normal atmosphere conditions. The $Gd_xSc_{3-x}N@C_{80}$, other educts, all solvents for chemical syntheses, fetal calf serum (FCS) and glutamine were purchased from Sigma-Aldrich, Germany or BACR, Karlsruhe, Germany. The chemicals used for peptide synthesis and purification were purchased from Roth, Germany. The solvents were of reagent grade and used without further purification. Amino acids, derivatives and coupling agents were purchased from Merck Bioscience, Germany. Cleavage reagents were from Fluka-Sigma-Aldrich, Buchs, Switzerland. RPMI cell culture medium was purchased from Invitrogen, Karlsruhe, Germany.

For the synthesis of the $Gd_xSc_{3-x}N@C_{80}$ -BioShuttle we used combined chemical methods: functional modules, the derivatized

endofullerene cargo as well as the peptide-based modules of the NLS address and the transmembrane transport component were added by solid phase peptide synthesis (SPPS).[39, 40] The ligation of the CA cargo was carried out with a special form of the Diels Alder Reaction (DAR), the Diels Alder Reaction with inverse electron demand (DAR_{inv}) which is the basis for the "Click Chemistry". The coupling of the $Gd_xSc_{3-x}N@C_{80}$ 8 cargo to the spacer follows established procedures, which after the reaction with the Reppe-anhydride acts as the dienophile. The diene (tetrazine) is introduced to the NLS module. Details of the preparation processes are given elsewhere.[41]

In order to facilitate the transfer of the $Gd_xSc_{3-x}N@C_{80}$ across cell membranes we used as cell penetrating peptide the fragment of the HIV-1-Tat protein 'GRKKRRQRRRPPQ'[42] representing residues 48-58.

The following conjugates were investigated (Table 1).

Modular structure of the used Gd-Cluster@-BioShuttle (13)			
Modules			
Cargo		Nuclear localization sequence	Cell Penetrating Peptide
MR-CA ^{*)}		NLS ^{**)}	CPP
$Gd_xSc_{3-x}N@C_{80}$			
	-C3-Spacer- ^{dienophile}	diene-PKKKRKV-C	GRKKRRQRRRPPQC
		-S-	-S- ^{***)}
(10)		(12)	
Dienophile-Compound		Diene-Compound	
	^{**)Magnetic resonance contrast agent}	^{**)Nuclear localization sequence}	^{***)Sulfur bridge}

Table 1: The modular structure of the Gd-Cluster@-BioShuttle. The module responsible for the transmembrane transport (right column) connects the NLS with the CPP via a cleavable sulfur bridge. The spacer harboring a dienophile-section between the NLS and the $Gd_xSc_{3-x}N@C_{80}$ acts as docking station for different substances, which possesses diene-structures.

Syntheses and conjugations of the modules for the Gd-Cluster@BioShuttle

Synthesis of the mixed metal nitride cluster fullerene $Gd_xSc_{3-x}N@C_{80}$

$Gd_xSc_{3-x}N@C_{80}$ ($x = 1, 2$) were produced by a modified Kraetschmer-Huffmann DC arc-discharge method which the addition of NH_3 (20 mbar) as described.[43, 44] Briefly, a mixture of Gd_2O_3 and Sc_2O_3 (99.9%, MaTeck GmbH, Germany) and graphite powder were used (molar ratio of **Gd** : **Sc** : **C** = **1** : **1** : **15**). After DC arc discharge, the soot was pre-extracted by acetone and further Soxhlet-extracted by CS_2 for 20 h. Fullerenes were isolated by a two-step HPLC. In the first step, running in a Hewlett-Packard instrument (series 1050), a linear combination of two analytical 4.6×250 mm Bucky-prep columns (Nacalai Tesque, Japan) was applied with toluene as eluent. The second-stage isolation was performed by recycling HPLC (Sunchrom, Germany) on a semi preparative Bucky-prep-M column (Nacalai Tesque, Japan) with toluene as eluent. An UV detector set to 320 nm was used for fullerene detection in both stages. The purity of the isolated products was tested by LD-TOF MS analysis running in both positive- and negative-ion modes (Biflex III, Bruker, Germany).

Synthesis of the diene compound N-(2-Aminopropyl)-4-(6-(pyrimidine-2-yl)-1,2,4,5-tetrazine-3-yl)benzamide (4)

4-(6-(pyrimidine-2-yl)-1,4-dihydro-1,2,4,5-tetrazine-3-yl)benzoic acid **3** was prepared from 2-pyrimidinecarbonitrile **1** and p-cyano benzoic acid **2** by reaction with 85% hydrazine. After purification by recrystallisation the dihydrotetrazine was then oxidized with nitric-acid to the tetrazine derivative following the known procedure[45] as shown in Figure 1 /scheme 1. The tetrazine derivative was converted with thionyl chloride under standard conditions to the corresponding acidic chloride. To a suspension of this acid chloride (2 mmol) in 20 ml CH_2Cl_2 , a solution of 3-amino butyric acid-tert-butyl-ester (2mmol) and Hunig's base (2 mmol) in 10 ml CH_2Cl_2 was slowly added at 0–5°C. The resulting deeply colored solution was maintained at room temperature for 4 h. Then the organic phase was washed with water, followed by 1N-HCl and again water. The organic layer was dried over Na_2SO_4 and evaporated. The resulting residue was chromatographed on silicagel by elution with chloroform/ethanol (9 : 1) and further purified by recrystallization from acetone. The yield was 50–70% depending on the quality of the carboxylic acid. ESI-MS: m/z 437.2 $[M]^+$. The Boc-protected derivative was treated with TFA (5ml) for 30 min at room temperature and isolated by evaporation to a solid residue **4** (ESI: m/z 337.2 $[M]^+$).

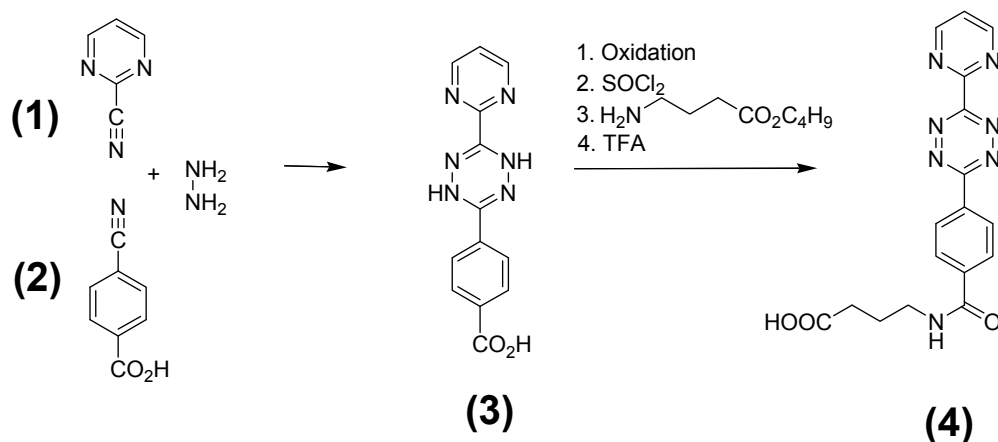


Figure 1. (Scheme 1) Demonstrates the synthesis steps of the N-(2-Aminopropyl)-4-(6-(pyrimidine-2-yl)-1,2,4,5-tetrazine-3-yl)benzamide **4** used as diene reaction partner.

Synthesis of the [tetracyclo-3,5-dioxo-4-aza-9,12-tridecadiene] dienophile (7) compound

The steps of the synthesis of the dienophile compound used for coupling the fullerene are carried out as follows: For synthesis of the dienophile compound 7 as educts were used the cyclooctotetraene (COT) 5 and maleic anhydride 6 as described in the synthesis prescript as follows: The tetracyclo-3,5-dioxo-4-aza-9,12-tridecadiene (TcT), called Reppe anhydride 7, was prepared from 4.4 g of (1Z,3Z,5Z,7Z)-cycloocta-1,3,5,7-tetraene 5 and 4.4 g maleic anhydride 6 in toluene as described by Reppe[46] as shown in Figure 2/Scheme 2.

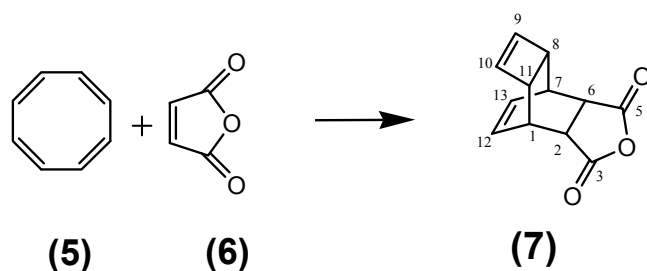


Figure 2. (Scheme 2) Illustrates the classical chemical reaction of the cyclooctotetraene (COT) 5 with maleic anhydride 6 to the resulting reaction product tetracyclo-3,5-dioxo-4-aza-9,12-tridecadiene called “Reppe anhydride” 7 used as dienophile reaction partner.

Ligation of the [tetracyclo-3,5-dioxo-4-aza-9,12-tridecadiene] (7) compound with the nitride cluster fullerene $Gd_xSc_{3-x}N@C_{80}$

This step describes the chemical modification of the nitride cluster fullerene 8. Therefore N-1,3.-diamino propane substituted glycine 9 reacts in a 1,3. cycloaddition with the fullerene derivative to the Boc-protected reaction product 10. Deprotection with TFA produces the free amine acting as which after reaction with the Reppe anhydride 7 formed the dienophile reactant 11, as illustrated later in Figure 4 /scheme 4.

The explicit synthesis steps as visualized in Figure 3/scheme 3, without the last step were conducted according the general synthetic strategy documented by Kordatos [47].

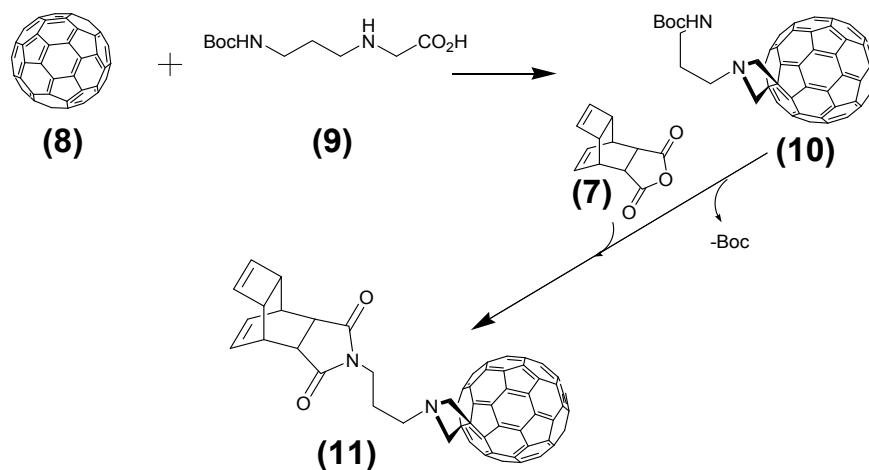


Figure 3. (Scheme 3) Shows the reaction of Reppe anhydride 7 after 1,3-dipolar cycloaddition reaction of the Boc protected N-1,3.-diamino propane linker substituted glycine 9 with the $Gd_xSc_{3-x}N@C_{80}$ 8. The product 11 acts as the dienophile reaction partner with diene tetrazine-NLS-S⁺S⁻-CPP conjugate 13 in the final DAR_{inv.} as pointed out in Figure 5/scheme 5).

Solid phase peptide synthesis (SPPS) of the NLS and CPP peptide modules

For solid phase syntheses of both, the NLS address peptide as well as of the CPP transport peptide, we employed the Fmoc-strategy in a fully automated multiple synthesizer (Syro II).[39] The synthesis was carried out on a 0.05 mmol Fmoc-Lys(Boc)-polystyrene resin 1% crosslinked and on a 0.053 mmol Fmoc-Cys(Trt)-polystyrene resin (1% crosslinked). As coupling agent 2-(1H-Benzotriazole-1-yl)-1,1,3,3-tetramethyluronium hexafluorophosphate (HBTU) was used. The last amino acid of the NLS-peptide was incorporated as Boc-Lys(COT)-OH. Cleavage and deprotection of the peptide resin were affected by treatment with 90% trifluoroacetic acid, 5% ethanedithiol, 2.5% thioanisole, 2.5% phenol (v/v/v/v) for 2.5 h at room temperature. The products were precipitated in ether. The crude material was purified by preparative HPLC on an Kromasil 300-5C18 reverse phase column (20 × 150 mm) using an eluent of 0.1% trifluoroacetic acid in water (A) and 60% acetonitrile in water (B). The peptides were eluted with a successive linear gradient of

25% B to 60% B in 40 min at a flow rate of 20 ml/min. The fractions corresponding to the purified peptides were lyophilized.

Ligation of the tetrazine diene compound N-(2-Amino-propyl)-4-(6-(pyrimidine-2-yl)-1,2,4,5-tetrazine-3-yl)benzamide (**4**) with the NLS-Cys peptide and coupling to the Cys-CPP via disulfide bridge formation.

The tetrazine diene compound **4** was attached to the N-terminus of the NLS sequence. Simultaneously a cysteine was appended to the C-termini of the NLS and the CPP peptides for disulfide bond formation between these modules. This enables the intracellular enzymatic cleavage and dissociation of the CPP from the NLS immediately after the passage into the cytoplasm. For the reaction the SH-groups of the CPP-Cys and of the tetrazine-NLS-Cys address module **12** were oxidized in the range of 2 mg × ml⁻¹ in a 20% DMSO water solution. Five hours later the reaction was completed. The progress of the oxidation to the resulting diene tetrazine-NLS-S[∧]S-CPP **13** (as shown in Figure 4/scheme 4) was monitored by analytical C18 reverse phase HPLC.

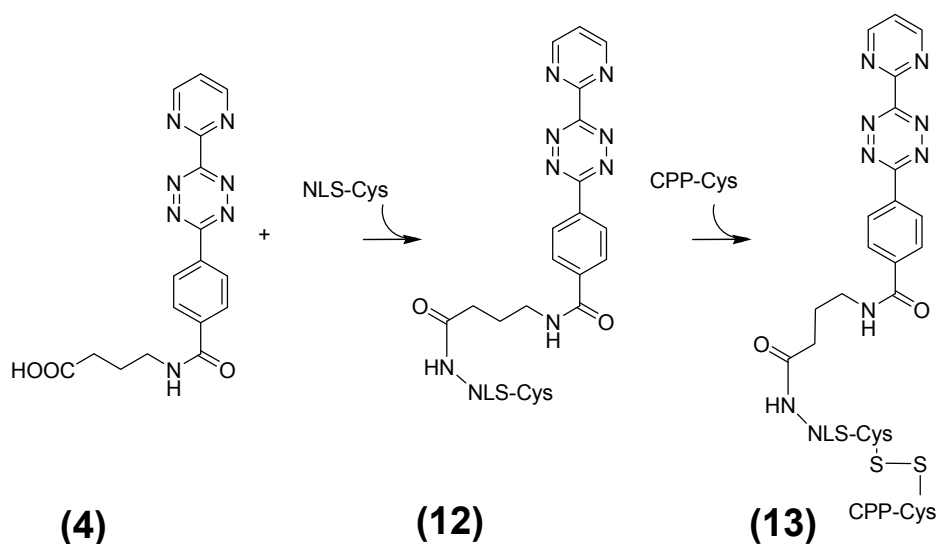


Figure 4. (Scheme 4) The resulting molecule **13** consists of the diene compound ligated by N-(2-aminopropyl)-4-(6-(pyrimidin-2-yl)-1,2,4,5-tetrazine-3-yl)benzamide linker to nuclear localization sequence (NLS) which in turn is covalently connected by disulfide bridge formation with the cysteines of the C-terminus of the cell penetrating peptide (CPP) and the NLS. This diene tetrazine-NLS-S[∧]S-CPP conjugate **13** was ligated with the functionalized MR imaging component GdSc₂@C_{80n} cargo **11** (Figure 3/scheme 3).

DAR_{inv} mediated ligation of the [TcT-N-propyl]-N-glycyl-GdSc₂@C_{80n} with the N-(2-Aminopropyl)-4-(6-(pyrimidine-2-yl)-1,2,4,5-tetrazine-3-yl)benzamide (4)-NLS-S⁺S-CPP to the Gd-cluster@-BioShuttle

Both compounds, the Gd-cluster-fullerene GdSc₂@C_{80n} linked with the [TcT-N-propyl]-N-glycyl dienophile **11** and the diene tetrazine-NLS-S⁺S-CPP

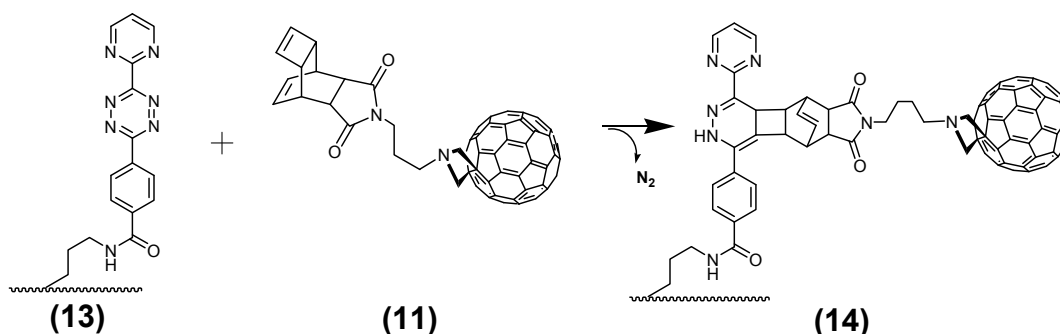


Figure 5. (Scheme 5) Depicts the Diels Alder inverse as the terminal ligation step to the Gd-cluster@-BioShuttle as final product **14** after purification ready for use in MR imaging studies.

Purification the Gd-cluster@-BioShuttle (**14**)

After ligation the product **14** was precipitated in ether and purified by preparative HPLC (Shimadzu LC-8A, Japan) on a YMC ODS-A 7A S-7 μ m reverse phase column (20 \times 250 mm), using 0.1% trifluoroacetic acid in water (A) and 60% acetonitrile in water (B) as eluent. The conjugate was eluted with a successive linear gradient, increasing from 25% to 60% B-eluent in 49 min at a flow rate of 10 ml/min. The fractions corresponding to the purified conjugate were lyophilized. Sequences of single modules as well as the complete bimodular construct were characterized with analytical HPLC (Shimadzu LC-10, Japan) using a YMC-Pack Pro C18 (150 \times 4.6mm ID) S-5 μ m, 120A column with 0.1% trifluoroacetic acid in water (A) and 20% acetonitrile in water (B) as eluent. The analytical gradient ranged from 5% (B) to 80% (B) in 35 minutes. The constructs were further characterized with laser desorption mass spectrometry (Finnigan, Vision 2000).

Cell culture

The human breast cancer cell line MDA-MB-231 was obtained from the American Type Culture Collection (ATCC). MDA-MB-231 cells were cultured routinely in RPMI-1640 (Invitrogen, Karlsruhe, Germany) supplemented with 10% FCS (Beckton & Dickinson, Germany). Cell cultures were kept under standard conditions (37°C, humidified atmosphere,

13 react in stoichiometrically equimolar amounts after dissolving in aqueous solution and storage at room temperature (as illustrated in Figure 5/scheme 5). The reaction is complete when the colour has changed from magenta to yellow. The Gd-cluster@-BioShuttle as a product **14** was isolated by lyophilization.

5% CO₂) and passaged 2 times a week.

MRI measurements

Protocol of the T1 magnetic resonance relaxometry

Different dilutions of the probes **14** (Gd-cluster@-BioShuttle) were prepared for T1 MR relaxometry of Gd-cluster@-BioShuttle. Gd-cluster@-BioShuttle (229 μ g) was dissolved in PBS containing 2% DMSO resulting in a concentration of 0.22 mmol/L (0.22 nmol/ μ L). The stock solution was diluted with Hank's solution to concentrations of (0.022 mmol/L) 0.022 nmol/ μ L, 0.0022 nmol/ μ L (2.2 μ mol/L) and 0.00022 nmol/ μ L (and 0.22 μ mol/L) respectively. The relaxivity was measured in 50 μ L of each probe. As references 50 μ L Hank's solution containing 2% DMSO and 50 μ L of Gd-DTPA (Magnevist®, 0.5 nmol/ μ L [0.5 mmol/L]) were used.

The MDA-MB-231 cells were incubated with 100 μ L of the respective solutions as well as Hank's solution containing 2% DMSO as a control. After 25 minutes, the solutions were removed from the cells, then cells were washed twice with Hank's solution and kept in Hank's solution containing 2% DMSO.

The T1 MR relaxometry measurements in a gelatine phantom of Gd-cluster@-BioShuttle in gelatine were performed with a saturation recovery turbo FLASH pulse sequence with different saturation recovery delays TI of 90, 200, 400, 800, 1200, 2000, 4000, and 7000 ms. The other imaging parameters were: TR

= 7160 ms; TE = 1,67 ms, 1 average; FOV = 150 mm; slice thickness = 4.5 mm; voxel size = $1.2 \times 1.2 \times 4.5$ mm³). From the series of images T1 relaxation times were calculated by a non-linear fit (Levenberg-Marquardt algorithm) of the signal amplitudes using the exponential saturation recovery relationship.

In the MDA-MB-231 cells morphologic MRI was carried out using a T1-weighted gradient echo sequence (TR, 600 ms; TE, 14 ms; averages, 3; FOV, 180 × 73 mm; slice thickness, 1.5 mm; flip angle, 90°), and a T2-weighted turbo spin echo sequence (TR, 1,070 ms; TE, 14 ms; average, 3; FOV, 180 × 73 mm; matrix, 256; slice thickness, 2 mm).

Cell viability

Human MDA-MB-231 breast adenocarcinoma cells were incubated with the Gd-cluster@-BioShuttle **14** in a concentration of 0.5 mM for 24, 48, and 72 hours. Untreated cells served as controls for the same time periods. The cell viability was assessed by a dye exclusion assay with trypan blue staining (0.4%) for 5 minutes. This dye exclusion assay is useful for a quick decision of cell toxicity. If an influence of the drug Gd-cluster@-BioShuttle on cell viability would be observed, a more sensitive assays for quantification like the MTT assay or flow cytometry could be used. Here we did not find a difference in the cellular phenotype between treated (0.5mM) and untreated control cells with the trypan blue assay.

Results and Discussion

We could not find a difference with dye exclusion assay between the control cells and the nitride-cluster endo-fullerenes treated cells until 72 hours.

Within this manuscript we would first like to illustrate the different chemical procedures in close context with 1. the solid phase peptide synthesis by Merrifield combined with 2. the protection group technology by Carpino for the synthesis of functional peptides, and 3. the synthesis of the nitride-cluster endo-fullerenes [Gd_xSc_{3-x}N@C₈₀ (x = 1, 2)] by the Kraetschmer-Huffmann DC arc-discharge method modified by Dunsch under addition of NH₃. 4. The synthesized components were combined using the Diels Alder Reaction inverse as an efficient ligation method for coupling the functional peptides as well as the nitride-cluster endo-fullerenes as a cargo. The second intention within this manuscript was to consider the MRI-measurements, described below as a basis for determining MRI tomographical signals in comparison to the commonly used MRI contrast agent (CA) Gd-DTPA.

MRI-Measurements in MDA-MB-231 breast adenocarcinoma cells

Recently, an endo-fullerene PEG- and hydroxy-functionalized [48], but no endo-fullerenes harbouring functionalizations of the Gd-cluster@-BioShuttles described in our manuscript, were documented.

In our measurements the concentrations of the Gd-cluster@-BioShuttle **14** 5 μmol Gd/kg were equivalent to 1/20 of a typical clinical dose (100 μmol Gd/kg) of Gd-DTPA.

In morphological T2 and T1 weighted sequences, Gd-cluster@-BioShuttle diluted 1:100 (0.0022 nmol/μL \triangleq 2.2 μM) and 1 : 1000 (0.00022 nmol/μL \triangleq 0.2 μ) appeared more hyperintense than the stock solution (0.2 nmol/μL) and the preceding dilution 1 : 10 which shows an averaged relaxation time slightly decreased from 1126.9 to 1101.1 ms. This finding corresponds to the quantification of T1 relaxation times, which was highest when Gd-cluster@-BioShuttle was diluted 1:1000 (T1 relaxation time of 1758 ms). For comparison, in 0.5 nmol/μL Gd-DTPA (Magnevist) a T1 relaxation time of 1090.5 ms was determined.

In advance: The way from a MRI tomographical signal is still far from a contrast agent in MRI. The first measurements could demonstrate: As shown here, our new intracellular MRI contrast agent (CA) could be a promising solution: We coupled a nitride-cluster endo-fullerene [Gd_xSc_{3-x}N@C₈₀ (x = 1, 2)] to the BioShuttle delivery system resulting in the Gd-cluster@-BioShuttle **14**. It was used to investigate whether an intracellular MR imaging is possible and to estimate the T1 relaxivity on MR (1.5 T).

Historically already in 1994 electron-spin-resonance and mass-spectrometry studies of metallofullerenes were documented by the Dunsch group and seemed to suggest a certain potential of metallofullerenes as appropriate candidates as MRI contrast agents.[49] Further MRI studies revealed a high proton relaxivity of Gd-fullerenols and a high signal enhancement at lower Gd concentrations [50] compared to the concentration of the commonly used Gd-DTPA [51] and other CAs like the Gd-BOPTA chelate gadobutrol [52] was documented. In our experiments we could confirm these MRI signal data in MDA-MB-231 breast cancer cells after incubation with the new CA Gd-cluster@-BioShuttle and like to point out that the investigated Gd-cluster@-BioShuttle diverges from the properties of the Gd-fullerenol developed by the Mikawa group. The former molecule is characterized by surface functionalization with hydroxyl groups, responsible for the water solubility, our molecule followed new strategies to circumvent the insolubility of fullerenes in biological fluids with

the aim to reach high local concentrations sufficient for formation of tomographical signals.[33]. After ligation of the CA $\text{GdSc}_2\text{@C}_{80n}$ as a cargo to the carrier molecule we obtain a conjugate referred as Gd-cluster@-BioShuttle **14** consisting of the modular component facilitating the transfer of the CA $\text{GdSc}_2\text{@C}_{80n}$ across the cell membrane and a short peptide which serves as an address sequence into the cell nucleus. After intracellular enzymatic cleavage and dissociation from the transport peptide follows the second step, the CA is being transported into the cell nuclei. This is mediated by the cell-immanent mechanism of the nuclear localization sequence (NLS)[32].

As demonstrated the paramagnetic water-soluble endo-metallofullerenes ($\text{GdSc}_2\text{@C}_{80}$), which have a T1 (longitudinal relaxation of protons in the magnetic field) shortening effect, can be used as a novel core material of MRI CAs.

The exceptional spectroscopic properties of endo-metallofullerenes responsible for phenomena as measured here are in the focus of the scientific research. They could result from properties like the non-planar π -electron system of sp^2 -hybrid orbitals of the carbon cage. In that case, π -electrons would follow an outward-directed electron shift along the p-orbital [53]. Therefore, the outward-facing orbital ellipsoid

increases in size, while the inward facing decreases. This results in a coupling of the electron spins with the nuclear spin of the rare earth element. In this scenario, the whereabouts of the unpaired d-electron of the respective molecule is also of importance. [54]. In the case of Sc@C_{82} the probability density function describes the unpaired d-electron in 84% of the cases near the metal. Therefore, the notation $\text{Sc}^{2+}\text{@C}_{82}$ much better describes the actual charge status [55]. The complexity of characterization of the metal-to-cage interactions is being supported by quantum chemical data, which describe a geometrical optimization of the cage [56, 57]. Thus, the strong electron-spin nuclear-spin dipole interactions result from a high density function of the unpaired d-electron near the metal.

These endohedral nitride clusters were synthesized and the evaluation of their paramagnetic properties is first described here. Surface functionalizations of the $\text{GdSc}_2\text{@C}_{80}$ are pivotal for the biomedical applications of endo-metallofullerenes such as $\text{GdSc}_2\text{@C}_{80}$ **8** (as shown in Figure 3/scheme 3). The important *in vitro* water proton relaxivity R1 (the effect on $1/T_1$) of Gd-fullerenes is significantly higher (> 500-fold, as shown in Figure A) than that of commercial MRI contrast agents, such as Gd-DTPA.

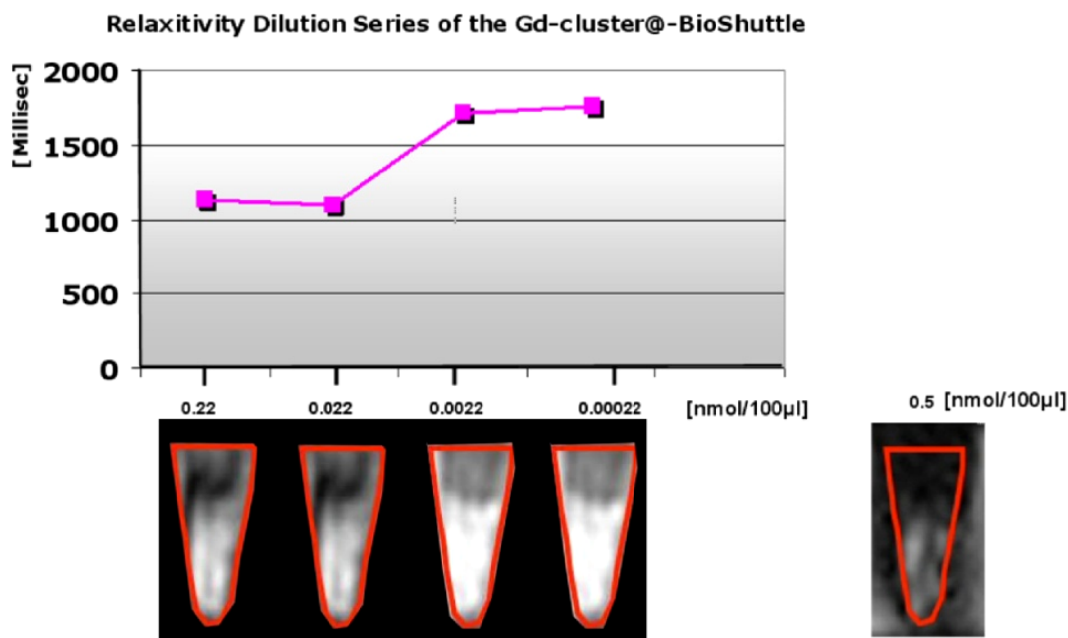


Figure A: illustrates a demonstration of the T1 weighted relaxation times. The ordinate of the graph in the upper part shows the relaxation times [msec], the axis of the abscissa represents the concentrations of the dilution series [nmol/100µL] of the Gd-cluster@-BioShuttle **14**. As a reference Gd-DTPA was used in a final concentration of 0.5 nmol/ 100 µL] the lower limiting concentration at which a barely tomographic signal is produced. The lower part of the figure reveals the corresponding tomographic signals in collected cells in reaction tubes. The Gd-DTPA control is in the lower panel on the right side.

Outlook

For stereotactical biopsies a contrast enhanced MRI with high spatial resolution is indispensable and depends on the increased signal intensity in observation of neo-angiogenesis, proliferation of endothelial cells [58] or of tumor tissue.[59] This difference in signal intensity between tumor cells and the interfaces of the surrounding healthy tissue is difficult to measure at present.[58] In general a good characterization of tissue by widely used 'old fashioned' Gd-complexes like Gd-DTPA is hardly possible. A determination of the distribution of grey-values and differential relaxation times are unsatisfactory so far, because radiation induced necrosis [58], vital tumor tissue and cerebral metastases are nearly undistinguishable.[51] Additionally, preclinical data suggest nephrotoxic properties induced by the commonly used Gd-based contrast media which hamper its use as an intracellular contrast agent.[60-62] Therefore a progress in the precision of therapy like the intensity-modulated radiation therapy (IMRT) and the use of heavy ions demands absolute reliability of new diagnostics and treatment planning for prostate and brain tumors. By the fact that the rare earth metals trapped inside of the carbon cage are isolated from the environment, the endo-metallofullerenes like the $GdSc_2@C_{80}$ **8** could be considered as ideal MRI contrast agents qualified for Molecular Imaging in MRT. Here we are at the beginning to evaluate the possibilities arising in the Molecular Imaging world.

Acknowledgments

This work was partially supported by Deutsche Krebshilfe, D-53004 Bonn; Grant Number: 106335. We thank Kristina Leger (IFW Dresden), Peter Lorenz and Heinz Fleischhacker (DKFZ) for technical assistance and for critical reading of the manuscript.

Conflict of Interest

The authors have declared that no conflict of interest exists.

References

- Kraetschmer W, Thumm M. Fullerene und Fullerite - neue Formen des Kohlenstoffs / Gyrotrons -Moderne Quellen für Millimeterwellen höchster Leistung. Paderborn: Schoeningh Verlag; 1996: 1-88.
- Gromov A, Ballenweg S, Giesa S, et al. Preparation and characterisation of C_{119} . Chem Phys Lett. 1997; 267: 460-6.
- Curl RF, Smalley RE, Kroto HW, et al. How the news that we were not the first to conceive of soccer ball C60 got to us. J Mol Graph Model. 2001; 19: 185-6.
- Smalley RE. Discovering the fullerenes. Rev Mod Phys. 1997; 69: 723-30.
- Curl RF, Kroto HW, Smalley RE. Nobel prize in chemistry for 1996. South African Journal of Chemistry-Suid-Afrikaanse Tydskrif Vir Chemie. 1997; 50: 102-5.
- Mattoussi H, Rubner MF, Zhou F, et al. Photovoltaic heterostructure devices made of sequentially adsorbed poly(phenylene vinylene) and functionalized C-60. Applied Physics Letters. 2000; 77: 1540-2.
- Funasaka H, Sakurai K, Oda Y, et al. Magnetic Properties of $Gd@C_{82}$ metallofullerene. Chemical Physics Letters. 1995; 232: 273-7.
- Chen C, Lieber CM. Isotope Effect and Superconductivity in Metal-Doped C_{60} . Science. 1993; 259: 655-8.
- Chiang LY, Swirczewski JW, Hsu CS, et al. Multi-hydroxy Additions onto C_{60} Fullerene Molecules. J Chem Soc, Chem Comm. 1992; : 1791-3.
- Chaudhary S, Lu H, Muller AM, et al. Hierarchical placement and associated optoelectronic impact of carbon nanotubes in polymer-fullerene solar cells. Nano Lett. 2007; 7: 1973-9.
- Narumi A, Kaga H, Miura Y, et al. Polystyrene microgel amphiphiles with maltohexaose. Synthesis, characterization, and potential applications. Biomacromolecules. 2006; 7: 1496-501.
- Comblin V, Gilsoul D, Hermann M, et al. Designing new MRI contrast agents: a coordination chemistry challenge. Coordination Chemistry Reviews. 1999; 186: 451-70.
- Caravan P, Ellison JJ, McMurry TJ, et al. Gadolinium(III) Chelates as MRI Contrast Agents: Structure, Dynamics and Applications. CHEM REV. 1999; 99: 2293-352.
- Ersoy H, Rybicki FJ. Biochemical safety profiles of gadolinium-based extracellular contrast agents and nephrogenic systemic fibrosis. J Magn Reson Imaging. 2007; 26: 1190-7.
- Anderson SA, Lee KK, Frank JA. Gadolinium-Fullerenol as a Paramagnetic Contrast Agent for Cellular Imaging. Invest Radiol. 2006; 41: 332-8.
- Bolskar RD, Benedetto AF, Husebo LO, et al. First soluble M@C-60 derivatives provide enhanced access to metallofullerenes and permit in vivo evaluation of $Gd@C-60[C(COOH)(2)](10)$ as a MRI contrast agent. Journal of the American Chemical Society. 2003; 125: 5471-8.
- Bolskar RD, Benedetto AF, Husebo LO, et al. First soluble M@C60 derivatives provide enhanced access to metallofullerenes and permit in vivo evaluation of $Gd@C60[C(COOH)2]10$ as a MRI contrast agent. J Am Chem Soc. 2003; 125: 5471-8.
- Okumura M, Mikawa M, Yokawa T, et al. Evaluation of water-soluble metallofullerenes as MRI contrast agents. Acad Radiol. 2002; 9 (Suppl 2): S495-S497.
- Tang J, Xing G, Zhao F, et al. Modulation of structural and electronic properties of fullerene and metallofullerenes by surface chemical modifications. J Nanosci Nanotechnol. 2007; 7: 1085-101.
- Ito Y, Fujita W, Okazaki T, et al. Magnetic properties and crystal structure of solvent-free $Sc@C_{82}$ metallofullerene microcrystals. Chemphyschem. 2007; 8: 1019-24.
- Yang S, Popov A, Kalbac M, et al. The isomers of gadolinium scandium nitride clusterfullerenes $GdxSc3-xN@C(80)$ ($x=1, 2$) and their influence on cluster structure. Chemistry. 2008; 14: 2084-92.
- Dunsch L, Yang S. Endohedral clusterfullerenes--playing with cluster and cage sizes. Phys Chem Chem Phys. 2007; 9: 3067-81.
- Weissleder R, Mahmood U. Molecular imaging. Radiology. 2001; 219: 316-33.
- Gambhir SS. Molecular imaging of cancer with positron emission tomography. Nat Rev Cancer. 2002; 2: 683-93.

25. Yap JT, Carney JP, Hall NC, et al. Image-guided cancer therapy using PET/CT. *Cancer J*. 2004; 10: 221-33.
26. Culver J, Akers W, Achilefu S. Multimodality molecular imaging with combined optical and SPECT/PET modalities. *J Nucl Med*. 2008; 49: 169-72.
27. Contag PR. Whole-animal cellular and molecular imaging to accelerate drug development. *Drug Discov Today*. 2002; 7: 555-62.
28. Li X, Wang J, An Z, et al. Optically imageable metastatic model of human breast cancer. *Clin Exp Metastasis*. 2002; 19: 347-50.
29. Massoud TF, Gambhir SS. Molecular imaging in living subjects: seeing fundamental biological processes in a new light. *Genes Dev*. 2003; 17: 545-80.
30. Heckl S, Debus J, Jenne J, et al. CNN-Gd(3+) Enables Cell Nucleus Molecular Imaging of Prostate Cancer Cells: The Last 600 nm. *Cancer Res*. 2002; 62: 7018-24.
31. Fawell S, Seery J, Daikh Y, et al. Tat-mediated delivery of heterologous proteins into cells. *Proc Natl Acad Sci U S A*. 1994; 91: 664-8.
32. Kalderon D, Roberts BL, Richardson WD, et al. A short amino acid sequence able to specify nuclear location. *Cell*. 1984; 39: 499-509.
33. Braun K, Peschke P, Pipkorn R, et al. A biological transporter for the delivery of peptide nucleic acids (PNAs) to the nuclear compartment of living cells. *J Mol Biol*. 2002; 318: 237-43.
34. Gorlich D, Mattaj JW. Nucleocytoplasmic transport. *Science*. 1996; 271: 1513-8.
35. Sauer J, Lang D, Mielert A. Reaktivitätsfolge Von Dienen Gegenüber Maleinsäureanhydrid Bei der Diels-Alder-Reaktion. *Angewandte Chemie-International Edition*. 1962; 74: 352.
36. Sauer J, Wiest H. Diels-Alder-Additionen Mit Inversem Elektronenbedarf. *Angewandte Chemie-International Edition*. 1962; 74: 353.
37. Braun K, Wiessler M, Ehemann V, et al. Treatment of glioblastoma multiforme cells with temozolomide-BioShuttle ligated by the inverse Diels-Alder ligation chemistry. *Drug Design, Development and Therapy*. 2008; 2: 289-301.
38. Pipkorn R, Waldeck W, Diding B, et al. Inverse-electron-demand Diels-Alder reaction as a highly efficient chemoselective ligation procedure: Synthesis and function of a BioShuttle for temozolomide transport into prostate cancer cells. *J Pept Sci*. 2009; 15: 235-41.
39. Merrifield RB. Solid Phase Peptide Synthesis. I The Synthesis of a Tetrapeptide. *J Americ Chem Soc*. 1963; 85: 2149-54.
40. Carpino LA, Ionescu D, El Faham A, et al. Complex polyfluoride additives in Fmoc-amino acid fluoride coupling processes. Enhanced reactivity and avoidance of stereomutation. *Org Lett*. 2003; 5: 975-7.
41. Waldeck W, Wiessler M, Ehemann V, et al. TMZ-BioShuttle--a reformulated temozolomide. *Int J Med Sci*. 2008; 5: 273-84.
42. Vives E, Brodin P, Lebleu B. A truncated HIV-1 Tat protein basic domain rapidly translocates through the plasma membrane and accumulates in the cell nucleus. *J Biol Chem*. 1997; 272: 16010-7.
43. Dunsch L, Yang S. Metal nitride cluster fullerenes: their current state and future prospects. *Small*. 2007; 3: 1298-320.
44. Yang S, Kalbac M, Popov A, et al. Gadolinium-based mixed-metal nitride clusterfullerenes Gd(x)Sc(3-x)N@C80 (x=1, 2). *Chemphyschem*. 2006; 7: 1990-5.
45. Wiessler M., Kliem C., Lorenz P., Mueller E., and Fleischhacker H. EU Patent: Ligation reaction based on the Diels Alder Reaction with invers electron demand. [EP 06 012 414.6]. 6-10-2006.
46. Reppe W, Schlichting O, Klager K, et al. Cyclisierende Polymerisation von Acetylen I. *Justus Liebigs Annalen der Chemie*. 1948; 560: 1-92.
47. Kordatos K, Da RT, Bosi S, et al. Novel versatile fullerene synthons. *J Org Chem*. 2001; 66: 4915-20.
48. Zhang J, Fatouros PP, Shu C, et al. High relaxivity trimetallic nitride (Gd3N) metallofullerene MRI contrast agents with optimized functionality. *Bioconj Chem*. 2010; 21: 610-5.
49. Bartl A, Dunsch L, Frohner J, et al. New Electron-Spin-Resonance and Mass-Spectrometric Studies of Metallofullerenes. *Chemical Physics Letters*. 1994; 229: 115-21.
50. Mikawa M, Kato H, Okumura M, et al. Paramagnetic water-soluble metallofullerenes having the highest relaxivity for MRI contrast agents. *Bioconj Chem*. 2001; 12: 510-4.
51. Just M, Higer HP, Vahldiek G, et al. [MR tomography in glioblastomas and cerebral metastases]. *Radiologe*. 1987; 27: 473-8.
52. Essig M. Protocol design for high relaxivity contrast agents in MR imaging of the CNS. *Eur Radiol*. 2006; 16 (Suppl 7): M3-M7.
53. Almeida MT, Pawlik T, Weidinger A, et al. Observation of Atomlike Nitrogen in Nitrogen-Implanted Solid C60. *Phys Rev Lett*. 1996; 77: 1075-8.
54. Nagase S, Kobayashi K. Metallofullerenes Mc82 (M=Sc, Y, and La) - A Theoretical-Study of the Electronic and Structural Aspects. *Chemical Physics Letters*. 1993; 214: 57-63.
55. Nagase S, Kobayashi K. The Ionization Energies and Electron-Affinities of Endohedral Metallofullerenes Mc(82) (M=Sc, Y, La) - Density-Functional Calculations. *Journal of the Chemical Society-Chemical Communications*. 1994; : 1837-8.
56. Kato T, Suzuki S, Kikuchi K, et al. ESR Study of the Electronic-Structures of Metallofullerenes - A Comparison Between La-At-C-82 and Sc-At-C-82. *Journal of Physical Chemistry*. 1993; 97: 13425-8.
57. Poirier DM, Knupfer M, Weaver JH, et al. Electronic and Geometric Structure of La-At-C-82 and C-82 - Theory and Experiment. *Physical Review B*. 1994; 49: 17403-12.
58. Earnest F, Kelly PJ, Scheithauer BW, et al. Cerebral astrocytomas: histopathologic correlation of MR and CT contrast enhancement with stereotactic biopsy. *Radiology*. 1988; 166: 823-7.
59. Kelly PJ, Daumas-Duport C, Kispert DB, et al. Imaging-based stereotaxic serial biopsies in untreated intracranial glial neoplasms. *J Neurosurg*. 1987; 66: 865-74.
60. Sieber MA, Lengsfeld P, Frenzel T, et al. Preclinical investigation to compare different gadolinium-based contrast agents regarding their propensity to release gadolinium in vivo and to trigger nephrogenic systemic fibrosis-like lesions. *Eur Radiol*. 2008; 18: 2164-73.
61. Sieber MA, Pietsch H, Walter J, et al. A preclinical study to investigate the development of nephrogenic systemic fibrosis: a possible role for gadolinium-based contrast media. *Invest Radiol*. 2008; 43: 65-75.
62. Grobner T. Gadolinium--a specific trigger for the development of nephrogenic fibrosing dermopathy and nephrogenic systemic fibrosis? *Nephrol Dial Transplant*. 2006; 21(4):1104-8.